Journal of the Serbian Chemical Society
JSCS-info@shd.org.rs • www.shd.org.rs/JSCS
J. Serb. Chem. Soc. *83* (3) 285–303 (2018)
JSCS–5075
UDC 519.677:66.095.252.091.7+546.163.3+547.388.4+547.772.2
Original scientific paper

A theoretical study on the regio- and stereoselectivity of [3+2] cycloaddition of 2-(trifluoroacetyl)vinyl ethyl ether to 2-arylidene-5-oxopyrazolidin-2-ium-1-ides

MINA HAGHDADI* and NASIM NAB

Department of Chemistry, Islamic Azad University, P. O. Box 755, Babol Branch, Babol, Iran

(Received 11 May, revised 23 July, accepted 28 August 2017)

Abstract: [3+2] Cycloaddition reactions of 2-(trifluoroacetyl)vinyl ethyl ether (**1**) to substituted and unsubstitued 2-arylidene-5-oxopyrazolidin-2-ium-1-ides (**2a**–**e**) were studied using density functional theory (DFT) methods at the cc-pVDZ level. The mechanistic details of these reactions, especially with respect to regio- and stereoselectivity, were analyzed. Analysis of the relative energies that are associated with the different reaction pathways indicated that the presence of the trifluoroacetyl group in the dipolarophile and substituents on the aryl ring in the dipolar have a remarkable effect on selectivity. In addition, it was found that the *ortho–endo* pathway with the lowest activation energy is preferred, which is in good agreement with the experimental data. Moreover, the elimination of ethanol from the [3+2] cycloadducts and the formation of bicyclic pyrazolidinones are explained in order to give a total description of the complete domino processes. The inclusion of solvent effects increased the activation energies and the exothermic character of the cycloadducts, but did not change the gas phase selectivity. The DFT-based reactivity indices clearly predicted the experimental regiochemistry.

Keywords: DFT study; trifluoroacetyl group; 2-arylidene-5-oxopyrazolidin-2--ium-1-ide; reactivity indices; cycloaddition reaction; bicyclic pyrazolidinone.

INTRODUCTION

[3+2] Cycloaddition (32CA) reactions are useful methods for the preparation of five-membered heterocycles, since they enable access to polyfunctional compounds with multiple asymmetric centers, usually with excellent stereo control.[1–3] The asymmetric cycloadditions of chiral nitrone, nitrile oxide, and azomethine ylides are well elaborated in many reports.[4–12]

The cyclic azomethine imine was first synthesized by Gotfresden in 1955,[13] and it was recognized as a [3+2] cycloaddition reaction in 1968.[14] Generally,

* Corresponding author. E-mail: mhaghdadi2@gmail.com
https://doi.org/10.2298/JSC170511099H

32CA reactions of cyclic chiral azomethine imines with various dipolarophiles were accompanied by high facial and *endo*/*exo*-selectivity and afforded the corresponding functionalized fused pyrazolidinones with a bridgehead N–N structural element.[14–18] The cycloaddition reactions of these dipolars were successfully employed with alkynes,[19] alkenes,[20–23] unsaturated ketones, aldehydes and esters[20,21] and in the case of asymmetric dipolarophiles, generally furnishing mixtures of regioisomeric heterocyclics.

During recent years, along with the development of click chemistry, 5-oxopyrazolidin-2-ium-1-ides, as cyclic azomethine imines, were efficiently used in cycloaddition reactions.[19,24] In 2011, Xin *et. al*.[25] prepared some bicyclic pyrazolidinone compounds (**7**) with anti-microbial and herbicidal activities[26] *via* the 32CA reactions of 2-(trifluoroacetyl)vinyl ethyl ether (TVE, **1**, unsaturated ketone) with some 5-oxopyrazolidin-2-ium-1-ides (**2**), in DMSO at room temperature. These 32CA reactions presented total regioselectivity and **1** as dipolarophile showed high activity (Scheme 1).

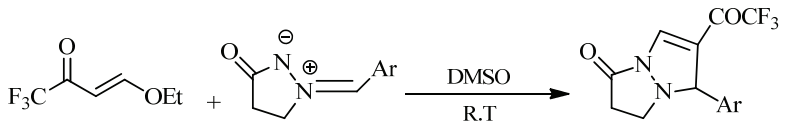

1 **2** **7**

Scheme 1. Experimental 32CA reaction of 2-(trifluoroacetyl)vinyl ethyl ether (TVE, **1**) with some 1-arylidene-5-oxopyrazolidin-2-ium-1-ides (**2**).

Some experimental and theoretical research has indicated that the trifluoromethyl group on a dipolarophile could considerably accelerate the cycloaddition reaction in the presence of a strong electron-withdrawing (EW) group.[27–29] Trifluoromethyl is an EW group, but it is not sufficient to activate ethylene efficiently. It acts through an inductive effect, *–I*, which increases the electrophilicity of ethylene, but does not cause a noticeable polarization of the π system. The formation of carbocyclic compounds with a trifluoromethyl group is interesting for the preparation of analogs of natural products due to their pharmacological activities.[30,31]

The interest in cyclic azomethine imines and the trifluoromethyl group in cycloaddition reactions were encouragements to perform this theoretical study on the regio- and stereoselectivity of these 32CA reactions. It should be noted that there are relatively few theoretical studies on 32CA reactions of azomethine imines with substituted alkenes in the literature.[32–34]

Herein, the results are presented of a density functional theory (DFT) study on 32CA reactions of TVE 1 with selected 5-oxopyrazolidin-2-ium-1-ides **2**, *i.e.*, 2-benzylidene-5-oxopyrazolidin-2-ium-1-ide (PY, **2a**), 2-(4-methoxybenzylid-

ene)-5-oxopyrazolidin-2-ium-1-ide (OMe-PY, **2b**), 2-(4-fluorobenzylidene)-5--oxopyrazolidin-2-ium-1-ide (F-PY, **2c**), 2-(4-bromobenzylidene)-5-oxopyrazol--idin-2-ium-1-ide (Br-PY, **2d**) and 2-(4-nitrobenzylidene)-5-oxopyrazolidin-2--ium-1-ide (NO2-PY, **2e**), which were experimentally reported by Xin *et al.*[25] First, the potential energy surfaces corresponding to all possible regio- and stereoselective pathways were investigated to establish the role of substituents and the trifluoromethyl group on the reactivity, and stereo-, and regioselectivity (see Scheme 2). Then, the global reactivity indices were defined within the conceptual DFT to find a structure/reactivity relationship based on the nucleophilic/ /electrophilic behavior of the reagents. Moreover, the local electrophilicity (ω_k) and nucleophilicity (N_k) indices with the Parr functions were used to explain the observed regioselectivity.

COMPUTATIONAL DETAILS

The ubiquitous B3LYP[35] hybrid functional has been the workhorse of quantum chemical studies on organic molecules for years.[36] It is well known that B3LYP can describe interactions in cycloaddition reactions. Recently, some functional, such as the MPWB1K,[37] have been proposed to investigate reaction energies, barrier heights and intermediates for 32CA reactions. For a comprehensive comparison of geometries, all species of the aforementioned 32CA reactions were optimized using both the B3LYP and MPWB1K exchange-correlation functionals. The cc-pVDZ basis set was used for full optimization with the B3LYP and MPWB1K methods. The electronic energies were corrected with zero-point energy (*ZPE*). All calculations were performed using Gaussian09.[38] The values of the relative energies, ΔE, were calculated based on the total energies of the stationary points. Relative enthalpies, ΔH, entropies, ΔS, and Gibbs energies, ΔG, at 298.15 K and 1 atm* were calculated using standard statistical thermodynamics.[39] Consequently, implicit solvent effects of dimethyl sulfoxide (DMSO) on the energies were taken into account through energy calculations using the polarizable continuum model (PCM), which was reported by the Tomasi group[40] within the framework of the self-consistent reaction field (SCRF).[41] The global electron density that was transferred (*GEDT*)[42] at the TSs was computed through a natural population analysis (NPA).[43]

The electronic structures of stationary points were analyzed by the natural bond orbital (NBO) method.[43] The global reactivity indices were estimated according to the equations proposed by Parr and Yang.[44] The global electrophilicity index, ω, which measures the stabilization in energy when the system acquires an additional electronic charge N from the environment is given by the following simple expression:[45]

$$\omega = \frac{\mu^2}{2\eta} \tag{1}$$

where μ is the electronic chemical potential and η is the chemical hardness.

Both μ and η may be evaluated in terms of the one-electron energies of the frontier molecular orbitals HOMO and LUMO, ε_H and ε_L,[44] using:

* 1 atm = 101325 Pa

$$\mu = (\varepsilon_H + \varepsilon_L)/2 \quad (2)$$

$$\eta = \varepsilon_L + \varepsilon_H \quad (3)$$

Recently, Domingo introduced an empirical (relative) nucleophilicity index, N,[46] based on the HOMO energies obtained within the Kohn Sham scheme[47] and defined as:

$$N = \varepsilon_{HOMO}(NU) - \varepsilon_{LUMO}(TCE) \quad (4)$$

Nucleophilicity is referenced to tetracyanoethylene (TCE) because this has the lowest HOMO energy in a large series of molecules already investigated in the context of polar cycloadditions. This choice allows a nucleophilicity scale of positive values to be conveniently handled. Recently, Domingo proposed two new Parr functions, an electrophilic, P_k^+, and a nucleophilic, P_k^-,[48] function, which were obtained through analysis of the Mulliken atomic spin density of the radical anion and cation by single-point energy calculations over the optimized neutral geometries using the unrestricted UB3LYP formalism for radical species. The local electrophilicity indices, ω_k,[48] and the local nucleophilicity indices, N_k,[48] were calculated using the following expressions:

$$\omega_k = \omega P_k^+ \quad (5)$$

$$N_k = N P_k^- \quad (6)$$

where P_k^+ and P_k^- are the electrophilic and nucleophilic Parr functions,[48] respectively. The transition states were verified by analysis of the intrinsic reaction coordinates (IRC) in both the forward and reverse directions.[49]

RESULTS AND DISCUSSIONS

The reaction between TVE (**1**) and a 1-arylidene-5-oxopyrazolidin-2-ium-1--ide compound (**2**) is comprised of two consecutive steps: first, the 32CA reaction of **1** with 5-oxopyrazolidin-2-ium-1-ide (**2**) occurred to produce trifluoroacetyl tetrahydro-1H,5H-pyrazolo[1,2-*a*]pyrazol-1-one stereoisomers **3**–**6** (Scheme 2), and then, the elimination process was accomplished to yield the final bicyclic pyrazolidinone compounds **7** (Scheme 3). In order to obtain mechanistic details, as well as to explain the experimentally observed complete regioselectivity in the formation of the bicyclic pyrazolidinones **7**, the present study is divided into three sections: I) the energetic aspects of stationary points and geometric parameters of TSs and their electronic structures in terms of bond orders and natural charges was studied for the 32CA reactions of **1** and 5-oxopyrazolidin-2-ium-1-ides **2a**–**e**, with special emphasis on the regio- and stereoselectivity; II) the elimination of ethanol from the primary cycloadducts was considered; III) finally, a DFT analyses based on the reactivity indices for the reactants were performed.

*Mechanistic details of the 32CA reactions of 2-(trifluoroacetyl)vinyl ethyl ether (**1**) and 5-oxopyrazolidin-2-ium-1-ides **2a**–**e***

In the cases considered here, four pathways are feasible for each reaction, namely two stereoisomeric and two regioisomeric reactive pathways. The two stereoisomeric approach modes of the carbonyl (C=O) group of **1** relative to the

sp^2 hybridized nitrogen of **2** produced two stereoisomeric, *endo* and *exo*, with two regioisomeric, *meta* and *ortho*, possibilities. The stereoisomeric pathways along the *ortho* routes correspond to the formation of C_1–C_5 and C_2–N_3, and along the *meta* routes correspond to C_2–C_5 and C_1–N_3 formation.

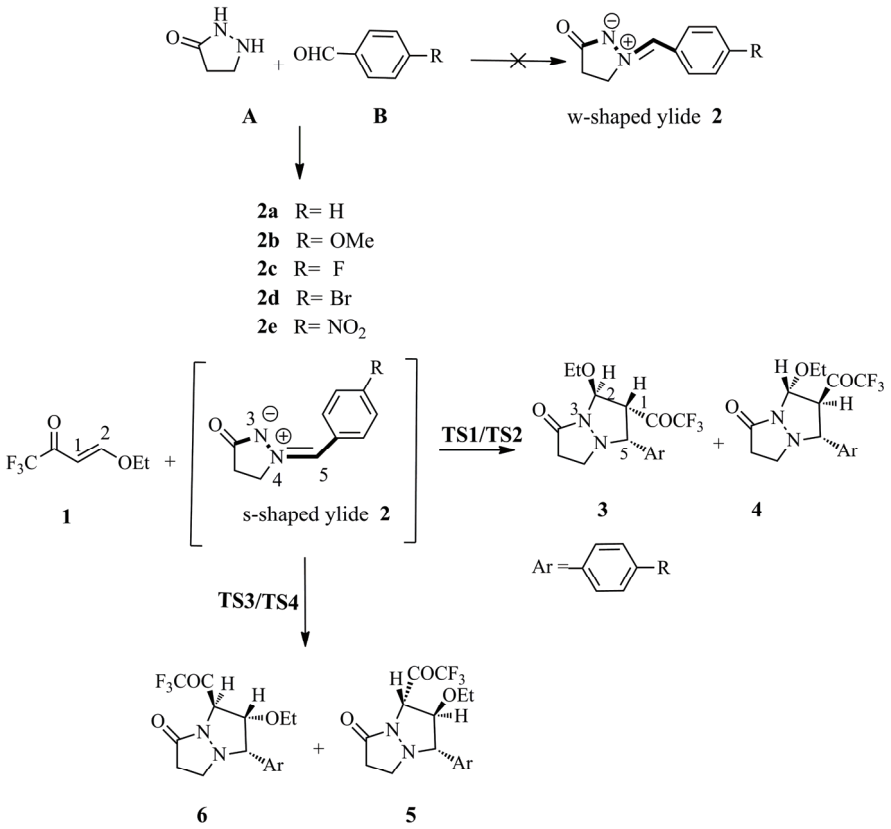

Scheme 2. The calculated possible reaction pathways for 32CA reactions between TVE (**1**) and 5-oxopyrazolidin-2-ium-1-ides **2a**–**e** at the B3LYP/cc-pVDZ level of theory.

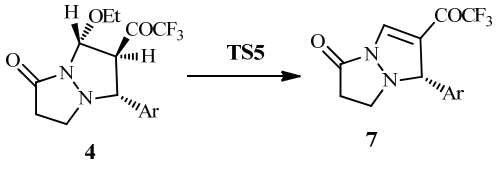

Scheme 3. Extrusion of ethanol from the *ortho–endo* cycloadducts **4**.

The analysis of the stationary points involved in these 32CA reactions indicated that they could occur through four TSs, TS1, TS2, TS3 and TS4, and four cycloadducts (CAs), **3**–**6** (Scheme 2). It should be noted that the 5-oxopyrazolidin-2-ium-1-ides **2** could result from the reaction of pyrazolidin-3-one (**A**) and some

aromatic aldehydes (**B**), which produce two types of pyrazolidinium ylide, *anti* (s-shape) and *syn* (w-shape, Scheme 2). The s-shape pyrazolidinium ylides energies are lower than those of the w-shape by 4.91 (**2a**), 6.14 (**2b**) 5.66 (**2c**), 5.77 (**2d**) and 5.29 (**2e**) kcal* mol^{-1}, which is in line with the product structure.

*Study of the 32CA reaction between TVE (**1**) and 1-benzylidene-5-oxopyrazolidin-2-ium-1-ide (PY, **2a**)*

Due to the unsymmetrical reagents, the 32CA reaction of **1** with **2a** can take place along four reaction pathways, involving the transition states **TS1a, TS2a, TS3a** and **TS4a**, and corresponding cycloadducts (CAs), **3a**, **4a**, **5a** and **6a** (Scheme 2). The stationary points of this reaction are presented in Scheme 2. The geometries of the TSs are presented in Fig. 1, and Fig. S-1 of the Supplementary material to this paper, and the atomic numbering, and the relative energies are summarized in Table I, and Table S-I of the Supplementary material.

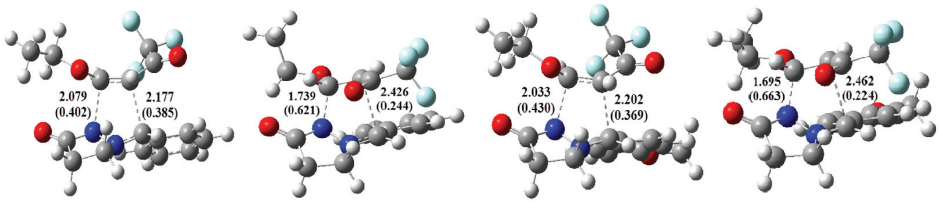

TS1a (*GEDT*=0.010) **TS2a** (*GEDT*=0.183) **TS1b** (*GEDT*=0.049) **TS2b** (*GEDT*=0.230)

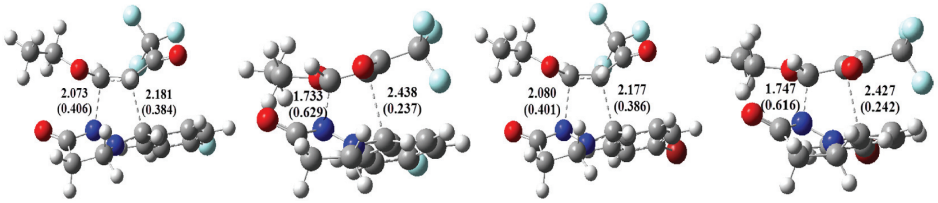

TS1c (*GEDT*=0.029) **TS2c** (*GEDT*=0.190) **TS1d** (*GEDT*=0.013) **TS2d** (*GEDT*=0.171)

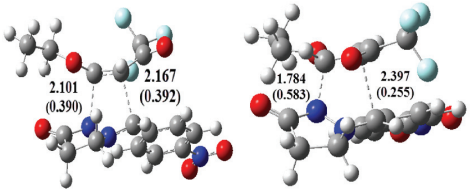

TS1e (*GEDT*=0.009) **TS2e** (*GEDT*=0.124)

Fig. 1. Optimized geometries of transition states involved in the 32CA reactions of **1** and **2a--e** along the *ortho* pathways at the B3LYP/cc-pVDZ level of theory. Bond distances are given in Å, Wiberg bond indices are given in parentheses and the global electron-density transfer (*GEDT, in e*) of the TSs are given (for a full comparison of the geometries, see the Supplementary material).

* 1 kcal = 4184 J

The activation energies associated with the four reactive pathways of the 32CA reaction between **1** and **2a** are 15.07 (**TS1a**), 4.32 (**TS2a**), 27.20 (**TS3a**) and 14.16 (**TS4a**) (Tables I and S-I). These energy barriers indicate that the *ortho* approach modes are more favorable than the *meta* ones by 12.13 and 9.84 kcal mol^{-1} for the *exo* and *endo* modes, respectively, leading to the formation of the *ortho* CAs **3a** and **4a**. Additionally, the *endo* approach mode in the *ortho* pathway is more favorable than the *exo* one by 10.75 kcal mol^{-1}. Thus, the large differences in the activation energies result in this reaction being completely stereo- and regioselective.

TABLE I. Calculated activation energies ($\Delta E^{\neq}$ / kcal mol^{-1}), reaction energies (ΔE_r / kcal mol^{-1}), activation Gibbs energies ($\Delta G^{\neq}$ / kcal mol^{-1}), activation enthalpies ($\Delta H^{\neq}$ / kcal mol^{-1}) and activation entropies ($\Delta S^{\neq}$ / cal mol^{-1} K^{-1} in the gas phase for the *ortho* pathways of the [3+2] cycloaddition between TVE (**1**) and 5-oxopyrazolidin-2-ium-1-ides **2a**–**e** at the B3LYP/cc-pVDZ level of theory. (For a full comparison of the energies, see the Supplementary material)

Reaction	TS	$\Delta E^{\neq}$	ΔE_r	$\Delta G^{\neq}$	$\Delta H^{\neq}$	$\Delta S^{\neq}$
1+**2a**→**3a**	**TS1a**	15.07	–16.36	28.91	15.06	–46.50
1+**2a**→**4a**	**TS2a**	4.32	–16.29	17.76	4.33	–45.06
1+**2b**→**3b**	**TS1b**	14.88	–15.65	27.91	14.87	–46.22
1+**2b**→**4b**	**TS2b**	3.34	–15.70	15.32	3.40	–43.33
1+**2c**→**3c**	**TS1c**	14.49	–16.65	27.07	14.48	–46.93
1+**2c**→**4c**	**TS2c**	3.24	–16.52	14.84	3.29	–44.52
1+**2d**→**3d**	**TS1d**	14.71	–16.55	27.26	14.72	–46.23
1+**2d**→**4d**	**TS2d**	3.41	–16.41	15.27	3.50	–43.57
1+**2e**→**3e**	**TS1e**	14.93	–16.31	28.10	14.98	–45.58
1+**2e**→**4e**	**TS2e**	3.63	–16.10	16.12	3.78	–42.96

As can be seen in Tables I and S-I, this reaction is exothermic with ΔE_r between –11.12 and –16.36 kcal mol^{-1} and so it could be considered irreversible. Furthermore, the formation of *ortho* CAs, **3a** and **4a** is more exothermic than *meta* CAs, **5a** and **6a,** by 5.22 and 5.17 kcal mol^{-1}, respectively.

The thermodynamic parameters, including changes in activation enthalpies, activation free energies and activation entropies as well as the reaction enthalpies, reaction free energies and reaction entropies were computed at 298.15 K and 1 atm and are given in Table I and Table S-II of the Supplementary material. A comparison between the relative activation enthalpies was associated with the four reactive pathways of the 32CA reaction of **1** with **2a** and indicates that the most favorable approach mode is the *ortho–endo* pathway which is associated with **TS2a** ($\Delta H^{\neq}$ = 4.33 kcal mol^{-1}). This was in line with the calculated activation energy. Moreover, analysis of the activation Gibbs energy changes showed that the *ortho–endo* reactive pathway is the consequence of the unfavorable negative activation entropy change associated with it, $\Delta S^{\neq}$ = –45.06 cal mol^{-1} K^{-1}. Addition of the entropic contribution to the enthalpy changed the

activation Gibbs energy change of the *ortho–endo* pathway to 17.76 kcal mol^{-1}. Hence, this 32CA reaction shows high stereoselectivity, as the activation Gibbs energy of **TS2a** is lower than of **TS1a** by 10.73 kcal mol^{-1}. The activation entropies for this 32CA reaction varied from –40.84 to –46.50 cal mol^{-1} K^{-1}, which raises the activation Gibbs energy from 17.76 to 34.07 kcal mol^{-1}.

The extent of the bond formation along a reaction pathway was provided by the concept of bond order (BO),[50] which has been used to study the molecular mechanism of chemical reactions and to evaluate the asynchronicity for formation processes. The BO values of C_1–C_5 and C_2–N_3 forming bonds along the *ortho* approach modes are 0.385 and 0.402 for **TS1a** and 0.244 and 0.621 for **TS2a**, respectively (Fig. 1). Furthermore, along the *meta* approach modes, the BO values of the C_1–N_3 and C_2–C_5 forming bonds are 0.352 and 0.202 for **TS3a**, and 0.214 and 0.551 for **TS4a**, respectively. These data indicate that in the TSs of the *ortho* pathway, the N–C forming bond is very advanced while in the *meta* pathway the C–C forming bond is generally more advanced than the N–C bond. Moreover, the most favorable *ortho–endo* TS is more asynchronous than the others, which is in agreement with the low activation energy.

Recently, Domingo *et al.* proposed the global electron-density transfer (*GEDT*)[42] concept for the TSs to analyze the polar nature of Diels–Alder and 32CA reactions. The *GEDT* concept is related to the electron density transfer that occurs from a nucleophile to an electrophile along a polar reaction,[42,51] and interestingly, a high correlation is found between the *GEDT* at the TSs and the polar character of these reactions. The *GEDT* was computed by sharing the natural charges for the TSs which were obtained by a natural bond orbital (NBO)[43] analysis between the nucleophilic and the electrophilic frameworks. The *GEDT* values for the TSs associated with the 32CA reaction of **1** with **2a** are given in Figs. 1 and S-1. The computed *GEDT* values that flux from **2a** to **1** are 0.010e for **TS1a**, 0.183e for **TS2a**, 0.037e for **TS**3a and 0.149e for **TS4a**, which indicate a low polar character for these 32CA reactions.

In order to establish the role of the trifluoromethyl group in the reactivity and selectivity of cycloaddition reactions, the 32CA reactions of **2a** with 4-ethoxybut-3-en-2-one (**1a**) and 1-ethoxy-4,4,4-triflourobut-1-ene (**1b**), were studied (Scheme 4). The relative energies are given in Table S-VI. As could be seen in Tables I and S-VI, the activation energy values of **1a** and **1b** with **2a** are higher than those obtained for **1**. The activation energies for the most favorable pathway (*ortho–endo*) of **2a** with **1a** and **1b** are 17.81 and 15.57 kcal mol^{-1}, respectively, which are higher than that for the most favorable pathway of **1** with **2a** (4.32 kcal mol^{-1}).

This shows that the inclusion of the carbonyl group in the α-position of the trifluoromethyl group in **1** apparently accelerates the cycloaddition reaction but modifies neither the complete regioselectivity, nor the high stereoselectivity.

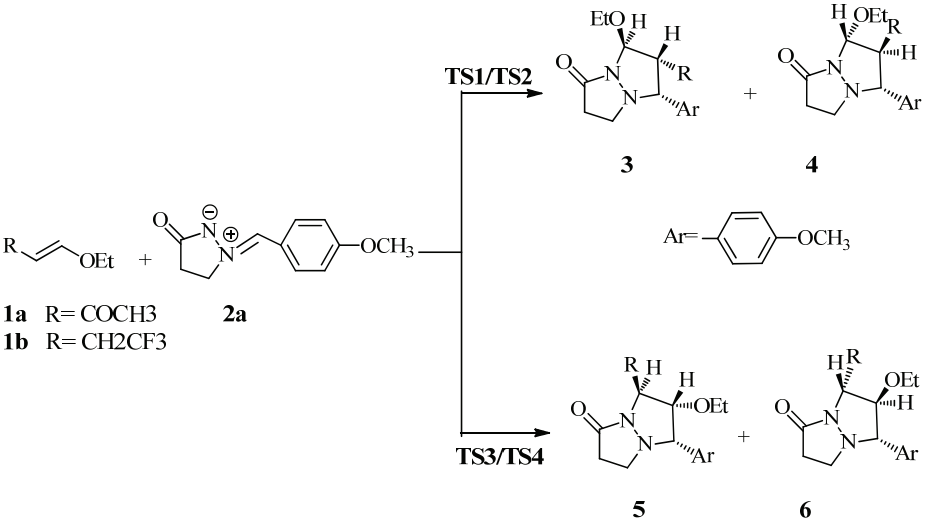

Scheme 4. The calculated possible reaction pathways for the 32CA reactions between 4-ethoxybut-3-en-2one (**1a**) and 1-ethoxy-4,4,4-triflourobut-1-ene (**1b**) with 5-oxopyrazolidin-2-ium-1-ide **2a** at the B3LYP/cc-pVDZ level of theory.

In order to compare the B3LYP energy results with the MPWB1K results, the stationary points of the most favorable pathways (*ortho*) from the B3LYP/cc-pVDZ level of theory were optimized at the MPWB1K/cc-pVDZ level.

The MPWB1K relative energies and Gibbs energies changes are given in Table S-V. A comparison of the relative energy changes indicates that the MPWB1K activation energies are less lower than those of the B3LYP method (between 1.44 to 1.80 kcal mol^{-1}) and the exothermicity was increased by around 10.0 kcal mol^{-1} as a consequence of lower stabilization of the reagents than of the TSs and cycloadducts. However, it could be concluded that the MPWB1K computations do not necessarily improve the B3LYP results.

Moreover, to investigate the solvent effect on the regio- and stereoselectivity of this reaction, the gas phase stationary points were studied in DMSO through single-point energy calculations at the B3LYP/cc-pVDZ level of theory. As could be seen in Table S-IV, the activation energies in DMSO associated with this 32CA reaction are higher than in the gas phase, because of the larger solvation of the reactants than the TSs. Therefore, while the inclusion of solvent effect increases the activation energies to 21.10 kcal mol^{-1} for **TS1a** and 7.99 kcal mol^{-1} for **TS2a,** the exothermic character decreased to –12.66 and –11.62

kcal mol^{-1} for **3a** and **4a**, respectively. In addition, the inclusion of the solvent effect has no effect on the regio- and stereoselectivity of this reaction, and the selectivity found in the gas phase is not changed.

*Study of the 32CA reactions between TVE (**1**) and electronically activated 5-oxo--pyrazolidin-2-ium-1-ides **2b**–**e***

Next, an analysis of the 32CA reactions of TVE (**1**) with substituted 5-oxo-pyrazolidin-2-ium-1-ides (**2b**–**e**) indicates that they can occur through four reactive pathways, namely all combinations of *ortho* or *meta* regioselectivity with *endo* or *exo* stereoselectivity. Thus sixteen TSs, **TS1**(**b–e**), **TS2**(**b–e**), **TS3**(**b–e**) and **TS4**(**b–e**) and the corresponding CAs, **3**(**b–e**), **4**(**b–e**), **5**(**b–e**) and **6**(**b–e**) were found and characterized for these 32CA reactions. The stationary points associated with these reactions are presented in Scheme 2, and the relative energies in the gas phase and DMSO are summarized in Tables I, S-I and S-IV.

As can be seen from Tables I and S-I, the energy barriers for all processes in the *ortho* pathways are lower than in *meta* ones, and the *endo* TSs are more stable than the *exo* ones. Hence, the *ortho–endo* pathways are the most favorable regio- and stereoselective pathways.

Some interesting conclusions could be drawn by comparing the 32CA reactions of **1** with **2b**–**e** at the B3LYP/cc-pVDZ level of theory:

I) While high stereoselectivity could be seen in the 32CA reaction of **1** with OMe-PY (**2b**) for the most favorable *ortho* regioisomeric pathways, $\Delta\Delta E^{\neq}$ = = 11.54 kcal mol^{-1}, low stability for the CAs were obtained for this reaction.

II) The energy barriers for the 32CA reaction of **1** with **2b**–**e**, in the more favorable pathways (*ortho*) are lower than those for the 32CA reaction of **1** with **2a**, which is a consequence of the effects of substituents on the aryl ring.

III) The presence of an ED or EW group on the aryl ring in **2c**–**e** increased the stereoselectivity, while the regioselectivites were decreased.

IV) While the *ortho* cycloadducts **3** and **4** are more stable than the *meta* ones (**5** and **6**) by about 5 kcal mol^{-1}, there is no significant difference in the stability of the *endo* and *exo* cycloadducts **3** and **4**.

V) All these cycloaddition reactions are exothermic, between –15.65 and –16.65 kcal mol^{-1} (in the *ortho* pathways) and hence, they could be considered irreversible.

The thermodynamic parameters of these 32CA reactions were calculated and are given in Tables I, S-I and S-II. It is interesting to note that the activation enthalpies for the *ortho–endo* pathways are the lowest, which is in agreement with the calculated activation energies. Additionally, these 32CA reactions are entropically unfavorable due to the steric bulk of the TSs and cycloadducts, which prevents their movement. However, the activation entropies in the *ortho–endo* pathways are less negative than in the other pathways. Consequently, the

activation Gibbs energy changes for the formation of the *ortho–endo* CAs are decreased and all 32CA reactions are spontaneous ($\Delta G_r<0$) and exothermic ($\Delta H_r<0$).

The geometries of all TSs in these 32CA reactions are shown in Figs. 1 and S-1. The lengths of the two forming bonds in the TSs are in the range of 2.16 to 2.20 Å (C_1–C_5) and 2.03 to 2.10 Å (C_2–N_3) for **TS1**, 2.39 to 2.46 Å (C_1–C_5) and 1.69 to 1.78 Å (C_2–N_3) for **TS2**, 1.94 to 1.97 Å (C_2–C_5) and 2.42 to 2.46 Å (C_1–N_3) for **TS3**, and 1.73 to 1.75 Å (C_2–C_5) and 2.33 to 2.40 Å (C_1–N_3) for **TS4**. An analysis of the lengths of the two forming bonds for these TSs reveals that the N–C bond length in the TSs associated with the most favorable *ortho* pathway, is shorter than the C–C one. However, for the *meta* pathway, the C–C bond is shorter than the N–C one. These geometric parameters suggest the shortest forming bond corresponds to that at the *β*-conjugated position of **1.** Meanwhile, there are highly asynchronous bond formation processes along the most favorable *ortho–endo* regioisomeric pathways but almost synchronous processes along the *ortho–exo* pathways.

The Wiberg index (*BO*) values of the forming bonds for the TSs are given in Figs. 1 and S-1. These *BO* values validate the main conclusions that were obtained from the analysis performed on the geometrical parameters. It could be seen that the electronic activation of 5-oxopyrazolidin-2-ium-1-ides **2** by the strong ED group $–OCH_3$ (**2b**) and the strong EW group $–NO_2$ (**2e**) does not produce any significant changes in the bond formation process of the geometries of the TSs. In addition, in the most favorable *ortho–endo* pathways, the corresponding *BO* values indicate that the formation of the C–N bond is more advanced than that of the C–C bond. Note that for the most favorable TSs, the analysis of the C–N and C–C *BO* values indicated an asynchronous bond formation process. Then, the extent of bond formation for TSs was confirmed with the calculated bond order (*BO*).

The electronic nature of the 32CA reaction of **1** with pyrazolidinium ylides **2b**–**e** was evaluated by computing the *GEDT* for the TSs associated with the four reactive pathways. The values of the *GEDT* are given in Figs. 1 and S-1. In the 32CA reactions of **1** with pyrazolidinium ylides **2b**–**d**, the *GEDT* of the most favorable TS, **TS2**, which fluxes from the ylide framework **2** to **1**, is between 0.171 and 0.230e. These values indicate that these processes have a small polar character and are in agreement with the computed low activation energies. Moreover, the presence of a strong withdrawing group ($–NO_2$) on aryl ring, **2e,** decreases the *GEDT* to 0.124e, with the low nucleophilic character of **2e** leading to this low value (see below).

The energy values of the solvent effect (DMSO) for these 32CA reactions are given in Tables I and S-I, and are shown not to modify the regio- and stereoselectivity that were found in the gas phase.

Elimination of ethanol

Experimentally, in all 32CA reactions of **1** with 5-oxopyrazolidin-2-ium-1-ides **2a**–**e**, 2-(trifluroacetyl)-2,3-dihydro-1H,5H-pyrazolo[1,2-*a*]pyrazol-1-one derivatives (**7a**–**e**) were obtained.[25] The formation of these products can only be explained by the initial formation of cycloadducts according to reaction *ortho–endo* pathways. However, it must be stressed that none of primary cycloadducts (**4a**–**e**) could be observed. Instead, they underwent a subsequent elimination of ethanol (Scheme 3). Consequently, a description is given of the elimination process in which the elimination of the ethanol from the cycloadducts **4a**–**e** leads to new fragments **7a**–**e**.

In all cases, concerted *cis* elimination of the hydrogen atom at C_1 and the ethoxy group at C_2 was calculated for the *ortho–endo* pathways. Relevant structural parameters for the corresponding transition states, as well as reaction energies, are shown in Fig. 2 and given in Tables II and S-III. As could be seen in Table II, the energy barriers for ethanol elimination are high, but if the high exothermicities of the formation of **4** are taken into account, the elimination TSs are lower than those for the cycloaddition TSs. Thus, the elimination step is the rate-determining step for the domino reactions. If the overall domino reaction is considered, the activation energies associated with the extraction of ethanol *via* TSs are 0.63 (**TS5a**), 9.75 (**TS5b**), 9.43 (**TS5c**), 9.77 (**TS5d**) and 9.42 (**TS5e**) kcal mol^{-1}; and the formation of the CAs **7** are exothermic by –29.67 (**7a**), –25.92 (**7b**), –28.28 (**7c**), –28.0 (**7d**) and –27.25 (**7e**) kcal mol^{-1}. The optimized geometries of the TSs involved in the elimination process of the CAs **4a**–**e** are given in Fig. 2. The lengths of the breaking and forming bonds of the TSs inv-

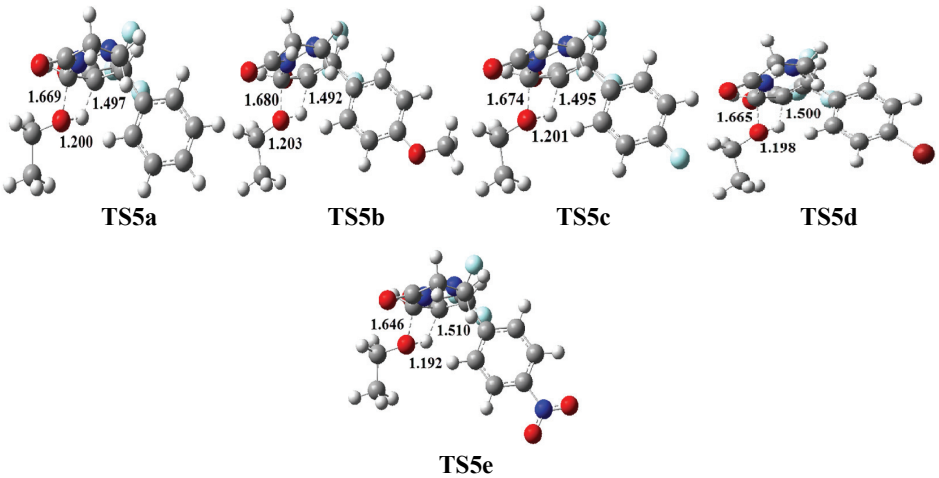

TS5a **TS5b** **TS5c** **TS5d** **TS5e**

Fig. 2. Optimized geometry of the transition states involved in the minimum energy pathway for the elimination reaction starting from the cycloadduct **4**.

olved in the ethanol elimination step are given in Fig. 2. The lengths of the C–O breaking bond are 1.497 (**TS5a**), 1.492 (**TS5b**), 1.497 (**TS5c**), 1.500 (**TS5d**) and 1.510 Å (**TS5e**). Furthermore, the lengths of C–H breaking bond are 1.669 (**TS5a**), 1.680 (**TS5b**), 1.674 (**TS5c**) 1.665 (**TS5d**) and 1.646 Å (**TS5**e), and of the H–O forming bonds, they are 1.200 (**TS5a**), 1.203 (**TS5b**), 1.201 (**TS5c**), 1.198 (**TS5d**) and 1.192 Å (**TS5e**). These data indicate that for **TS5e**, the ethanol elimination process is more advanced than for the others.

TABLE II. Calculated relative activation energies ($\Delta E^{\neq}$ / kcal mol^{-1}), reaction energies (ΔE_r / kcal mol^{-1}), activation Gibbs energies ($\Delta G^{\neq}$ / kcal mol^{-1}), activation enthalpies ($\Delta H^{\neq}$ / kcal mol^{-1}) and activation entropies ($\Delta S^{\neq}$/ cal mol^{-1} K^{-1}) in gas phase for the elimination of ethanol from cycloadduct **4** at the B3LYP/cc-pVDZ level of theory

Reaction	TSs	$\Delta E^{\neq}$	ΔE_r	$\Delta G^{\neq}$	$\Delta H^{\neq}$	$\Delta S^{\neq}$
4a→7a	**TS5a**	26.92	–13.38	35.42	26.59	–47.87
4b→7b	**TS5b**	25.45	–10.22	33.91	27.88	–46.57
4c→7c	**TS5c**	25.95	–11.76	32.33	26.23	–48.25
4d→7d	**TS5d**	26.18	–11.59	33.84	27.68	–47.48
4e→7e	**TS5e**	25.52	–11.15	32.97	26.36	–46.56

All the elimination steps are spontaneous (ΔG_r<0), exothermic (ΔH_r<0) and favored by entropy (ΔS_r>0), which indicate that the formed cycloadducts **4a** and **4e** are unstable and readily convert to **7a**–**e** (see Table S-III). The elimination step following the 32CA reaction occurs spontaneously without the presence of any other reagent.

DFT-based reactivity indices analysis

Recent studies devoted to DA and 32CA reactions have shown that analysis of the reactivity indices defined within the context of the conceptual DFT[52,53] was a powerful tool to understand the reactivity in polar cycloadditions. The DFT reactivity indices, namely, the electronic chemical potential, μ, hardness, η, electrophilicity, ω, and nucleophilicity, N, indices of **1** and the 5-oxopyrazolidin-2--ium-1-ides **2a**–**e** are given in Table III.

The electronic chemical potential of TVE (**1**), μ = –4.43, is lower than those of the 5-oxopyrazolidin-2-ium-1-ides **2a–2d**, μ = –3.99 to –3.34, indicating that along a polar cycloaddition reaction, the *GEDT* will occur from the pyrazolidinium ylides (**2a**–**d**) toward the electron deficient **1.** In contrast, the electronic chemical potential of NO2-PY **(2e**), in which the phenyl substituent has an EW group (–NO_2) at the *para* position of the aryl ring, μ = –4.604, is lower than the electronic chemical potential of **1**, stressing that the *GEDT* will occur from **1** toward **2e**, in clear agreement with the *GEDT* for the TSs.

The nucleophilicity index of PY (**2a**) is high, with N = 3.46 eV and hence, it is classified as a strong nucleophile within the nucleophilicity scale.[54] In contrast, a carbonyl group at the N_3 nitrogen atom (see Scheme 2 for atom numbering)

and a phenyl group at the C_1 carbon atom of **2a** give a high electrophilicity index, ω = 2.00 eV, making it possible to classify this species as a strong electrophile on the electrophility scale.[55] Consequently, it is expected that it will react toward nucleophilic and electrophilic dipolarophiles in 32CA reactions *via* a zw-type mechanism.[56]

TABLE III. HOMO energies / au, LUMO energies / au, electronic chemical potential (μ / eV), chemical hardness (η / eV), global electrophilicity (ω / eV) and nucleophilicity (N/ eV) for the reactants obtained at the B3LYP/cc-pVDZ level of theory

Species	E_{HOMO}	E_{LUMO}	μ	η	ω	N
1	–0.25715	–0.06967	–4.431	5.083	1.930	2.183
1a	–0.23567	–0.03700	–3.692	5.380	1.267	2.761
1b	–0.22985	–0.01369	–2.901	5.857	0.717	2.918
2a	–0.20982	–0.07373	–3.844	3.690	2.001	3.461
2b	–0.16828	–0.07821	–3.342	2.442	2.287	4.593
2c	–0.21106	–0.07500	–3.878	3.689	2.038	3.433
2d	–0.21389	–0.08102	–3.998	3.603	2.218	3.357
2e	–0.23017	–0.10941	–4.604	3.274	3.237	2.915

More interesting results are found with an ED group (–OCH_3) or an EW group (–F, –Br, –NO_2) at the *para* position of the aryl ring. In general, the methoxy group on **2b** increases the electrophilicity, ω = 2.29 eV, and increases the nucleophilicity, N = 4.56 eV, compared with **2a**. Similarly inclusion of an EW group (–F, –Br, –NO_2) on the aryl ring, increases the electrophilicity indices to 2.04 (**2c**), 2.22 (**2d**) and 3.24 (**2e**) eV, which classifies them as very strong electrophiles, but decreases the corresponding nucleophilicity N indices to 3.43 (**2c**), 3.36 (**2d**), and 2.92 (**2e**) eV. In spite of these facts, they remain classified as strong nucleophiles. Consequently, it is expected that they could participate in 32CA reactions with a polar character.

Furthermore, **1** presents both high electrophilicity, ω = 1.93 eV, and high nucleophicity, N = 2.18 eV, and hence, could be classified both as a moderate electrophile and nucleophile within the electrophilicity[55] and nucleophilicity[54] scales. The above results indicate that along electrophilic/nucleophilic interactions, the more favorable ones would be between **1**, acting as an electrophile, and 5-oxopyrazolidin-2-ium-1-ides **2a**–**d**, acting as nucleophiles and also between **2e** acting as an electrophile and **1** acting as a nucleophile.

In contrast, by comparing the electrophilic activation of TVE (**1**), ω = 1.93 eV, with 4-ethoxybut-3-en-2-one (**1a**), ω = 1.27 eV, and 1-ethoxy-4,4,4-triflouro-but-1-ene (**1b**), ω = 0.72 eV, it is clear that low electrophilicity indices of **1a** and **1b** are coupled with low reactivity in polar processes. Consequently, the strong electrophilic character of **1** accounts for the low activation energy computed for these 32CA reactions.

The relationship between the difference in electrophilicity for the 1,3--dipole/dipolarophile pair, $\Delta\omega$, and the static polarity may be a useful tool to describe the electronic pattern expected for the TSs involved in the 32CA reaction, describing them as low polar ($\Delta\omega$ small) or high polar ($\Delta\omega$ large) mechanisms.[57] The high $\Delta\omega$ between **1** and **2e**, 1.31 eV, shows a polar character for this 32CA reaction. The values of $\Delta\omega$ for the 32CA reactions of **1** with 3-oxopyrazolidinium ylides **2a**–**d**, decreased to 0.07 eV for **1**+**2a**, 0.36 eV for **1**+**2b,** 0.11 eV for **1**+**2c** and 0.29 eV for **1**+**2d**. Moreover, the charge transfer pattern for the 32CA processes may be estimated using the values of electronic chemical potential and chemical hardness for the reactants. Thus, the highest *GEDT* (0.233 e in Fig. 1) and the largest chemical potential difference ($\Delta\mu$ = 1.09 eV) occur in the 32CA reaction of **1** with **2b**, and a simultaneous decrease in the chemical hardness of 2.44 eV was observed, which is associated with a low resistance to charge transfer. It is worth noting that the minimum *GEDT* value is obtained along the high synchronous TS, **TS1**.

Along a polar reaction involving the participation of non-symmetric reagents, the most favorable reactive pathway is that involving the initial two-center interaction between the most electrophilic center of the electrophile and the most nucleophilic center of the nucleophile in all of reagents.[46] Recently, Domingo *et al.* proposed the electrophilic P_k^+ and nucleophilic P_k^- Parr functions, derived from the changes of the electron density from the nucleophile to the electrophile, as powerful tools in the study of the local reactivity in polar processes.[48] Hence, in order to characterize the most nucleophilic and the most electrophilic centers of the species involved in these 32CA reactions, the nucleophilic P_k^- Parr functions of **2a**–**d,** the electrophilic P_k^+ Parr function of **2e** and the electrophilic P_k^+ and the nucleophilic P_k^- Parr functions of dipolarophile **1** were analyzed. The Parr functions were computed based on the Mulliken atomic spin density analysis and the local electrophilicity indices (ω_k) and local nucleophilicity indices (N_k) were computed for C_1, C_2, N_3, and C_5 atoms of the dipolarophile **1** and **2a**–**e**, which are given in Table IV (see Scheme 2 for atomic numbering).

Analysis of the electrophilic P_k^- Parr functions of **1** indicate that the C_2 atom is the most electrophilic center of this species, P_k^+ = 0.497, and with a maximum local electrophilicity index, ω_k, of 1.22 eV, which decreases to 0.23 eV at the C_1 atom. Moreover, an analysis of the nucleophilic P_k^- Parr functions of PY (**2a**) indicate that the N_3 atom is more nucleophilically activated, P_k^- = 0.58, compared to the C_5 carbon, P_k^- = 0.13, while the corresponding local nucleophilicity indices, N_k, are N_{N3} = 2.01 eV and N_{C5} = 0.47 eV. Therefore, the most favorable electrophile–nucleophile interaction along the nucleophilic attack of **2a** to **1** will occur between the most nucleophilic center of PY (**2a**), the N_3 atom, and the

most electrophilic center of **1**, the C_2 atom, leading to the formation of CAs **3a** and **4a**, which is in agreement with experimental observations.[25] The same results were obtained for the 32CA reactions of **1**+**2b**, **1**+**2c** and **1**+**2d.** In contrast, in the 32CA reaction of **1** with NO2-PY (**2e**), the most nucleophilic center of **1** is the C_1 atom with the maximum value, $P_k^- = 0.59$ eV, and the local nucleophilicity index is $N_{C1} = 1.29$ eV. Moreover, the electrophilic P_k^+ Parr functions of **2e** indicate that the C_5 atom is the most electrophilic center of this species, with $P_k^+ = 0.17$ and the corresponding local electrophilicity values is $\omega_{C5} = 0.22$ eV. Hence, the most favorable two-center interaction occurs between the C_1 atom of **1** and the C_5 atom of **2e**, leading to the formation of the **3e** and **4e** stereoisomers, which is in agreement with the experimental findings.[25]

TABLE IV. The Parr functions ($P_k^{\pm}$ / au), local electrophilicity indices (ω_k / eV) and local nucleophilicity (N_k / eV) at the reactive sites of the reactants calculated at the B3LYP/cc-pVDZ level of theory

Species	k	P_k^+	P_k^-	ω_k	N_k
1	C1	0.120	0.592	0.232	1.292
	C2	0.497	0.018	1.223	0.064
2a	N3	0.034	0.582	0.068	2.014
	C5	0.210	0.135	0.420	0.467
2b	N3	0.027	0.533	0.061	2.431
	C5	0.245	0.037	0.560	0.168
2c	N3	0.034	0.573	0.069	1.967
	C5	0.223	0.122	0.454	0.419
2d	N3	0.047	0.558	0.104	1.873
	C5	0.166	0.109	0.368	0.366
2e	N3	0.018	0.588	0.058	1.714
	C5	0.167	0.193	0.217	0.562

CONCLUSIONS

The regio- and stereochemistry of 1,3DC reactions between 2-(trifluoro-acetyl)vinyl ethyl ether, TVE (**1**), with 5-oxopyrazolidin-2-ium-ides **2a**–**e** were investigated at the B3LYP/cc-pVDZ and MPWB1K/cc-pVDZ level of theory in the gas phase and a solvent (DMSO). Generally, these cycloadditions proceed through a one-step but asynchronous reaction mechanism. The lowest activation energies are obtained for *ortho–endo* pathway in all cases. Moreover, the primary cycloadducts could never be isolated but were converted into (trifluroacetyl)-2,3--dihydro-1H,5H-pyrazolo[1,2-*a*]pyrazol-1-one derivatives (**7**) by subsequent elimination of ethanol. The energy barrier for the elimination step is slightly higher than the cycloaddition step and is extremely exothermic. The inclusion of the solvent effect increased the activation energy and decreased the exothermic character of these 32CA reactions because of the larger solvation of reagents than transition states and cycloadducts. Analysis of the DFT global reactivity indices

and the Parr functions of the reactants allow an explanation of the regioselectivities of these 32CA reactions to be provided.

SUPPLEMENTARY MATERIAL

Additional calculated data are available electronically at the pages of the journal website: http://www.shd.org.rs/JSCS/, or from the corresponding author on request.

Acknowledgement. The authors wish to acknowledge Dr Louise S. Price, University College London, UK, for reading the manuscript and providing valuable suggestions.

ИЗВОД

ТЕОРИЈСКО ПРОУЧАВАЊЕ РЕГИО- И СТЕРЕОСЕЛЕКТИВНОСТИ [3+2] ЦИКЛОАДИЦИЈА 2-(ТРИФЛУОРАЦЕТИЛ)ВИНИЛ-ЕТИЛ-ЕТРА СА 2-АРИЛИДЕН-5-ОКСОПИРАЗОЛИДИН-2-ИЈУМ-1-ИДИМА

MINA HAGHDADI и NASIM NAB

Department of Chemistry, Islamic Azad University, P. O. Box 755, Babol Branch, Babol, Iran

[3+2] циклоадиционе реакције 2-(трифлуорацетил)винил-етил-етра (**1**) са супституисаним и несупституисаним 5-оксопиразолидин-2-ијум-1-идима **2a**–**e** проучаване су коришћењем метода теорије функционала густине (DFT) на cc-pVDZ нивоу. Анализирани су механистички детаљи ових реакција, посебно у погледу на регио- и стереоселективност. Анализа релативних енергија придружених различитим реакционим путевима указује да присуство трифлуорацетил групе у диполарофилу и супституенти на арил прстену приметно утичу на селективност. Такође је нађено да је преферисан *ortho–endo* пут са најнижом активационом енергијом, што је у доброј сагласности са експерименталним подацима. Штавише, елиминација етанола из [3+2] циклоадуката и формирање бицикличних пиразолидинона су објашњени како се дао потпун опис укупних домино процеса. Укључивање ефеката растварача повећава активационе енергије и егзотермни карактер циклоадуката, али не мења селективност из гасне фазе. Индекси реактвности засновани на DFT јасно предвиђају експерименталну региохемију.

(Примљено 11. маја, ревидирано 23. јула, прихваћено 28. августа 2017)

REFERENCES

1. A. Padwa, *1,3-Dipolar Cycloaddition Chemistry*, A. Padwa, Ed., Wiley, New York, 1984, Vol. 1, p. 732
2. V. K. Gothelf, K. A. Jørgensen, in *Synthetic Applications of 1,3-Dipolar Cycloaddition Chemistry toward Heterocycles and Natural Products*, A. Padwa, W. H. Pearson, Eds., Wiley, Hoboken, NJ, 2003
3. R. Grashey, in *1,3-Dipolar Cycloaddition Chemistry*, A. Padwa, Ed., Wiley, New York, 1984
4. B. Stanovnik, *Tetrahedron* **47** (1991) 2925
5. M. Žličar, B. Stanovnik, M. Tišler, *Tetrahedron* **48** (1992) 7965
6. M. Žličar, B. Stanovnik, M. Tišler, *J. Heterocycl. Chem.* **30** (1993) 1209
7. T. Oishi, K. Yamagushi, N. Mizuno, *Chem. Lett*. **39** (2010**)** 1057
8. B. Stanovnik, B. Jelen, C. Turk, M. Žličar, J. Svete, *J. Heterocycl. Chem.* **35** (1998) 1187
9. H. Dorn, *Chem. Heterocycl. Compd. USSR* **3** (1981), and references cited therein.
10. R. M. Claramunt, J. Elguero, *Org. Prep. Proced. Int.* **23** (1991) 273
11. R. J. Ternansky, S. E. Draheim, *Tetrahedron* **48** (1992) 777

12. J. Svete, A. Prešeren, B. Stanovnik, L. Golič, S. Golič Grdadolnik, *J. Heterocycl. Chem*. **34** (1997) 1323
13. W. O, Gotfresden, S. Vargedal, *Acta Chem. Scand.* **9** (1955) 1498
14. H. Dorn, A. Otto, *Chem. Ber*. **101** (1968) 3287
15. F. Roussi, A. Chauveau, M. Bonin, L. Micouin, H. P. Husson, *Synthesis* **2000** (2000) 1170
16. A. Chauveau, T. Martens, M. Bonin, L. Micouin, H. P. Husson, *Synthesis* **2002** (2002) 1885
17. R. J. Ternansky, S. E. Draheim, *Tetrahedron Lett.* **31** (1990) 2808
18. R. E. Holmes, D. A. Neel, *Tetrahedron Lett.* **31** (1990) 5570
19. H. Dorn, *Tetrahedron Lett.* **26** (1985) 5126
20. K. Yoshimura, K. Yamaguchi, N. Mizuno, *Chem. Lett.* **39** (2010) 1087
21. W. Chen, X. H. Yuan, R. Li, W. Du, Y. Wu, L. S. Ding, Y. C. Chen, *Adv. Synth. Catal*. **348** (2006) 1822
22. M. P. Sibi, D. Rane, L. M. Stanley, T. Soeta. *Org. Lett.* **10** (2008) 2974
23. K. Tanaka, T. Kato, Y. Ukaji, K. Inomata, *Heterocycles* **80** (2010) 893
24. a) R. Shintani, T. Hayashi, *J. Am. Chem. Soc.* **128** (2006) 6331; b) N. D. Shapiro, Y. Shi, F. D. Toste, *J. Am. Chem. Soc.* **131** (2009) 11655; c) S. Chassaing, A. Alix, T. Boningari, K. Sani Souna Sido, M. Keller, P. Kuhn, B. Louis, J. Sommer, P. Pale, *Synthesis* **2010** (2010) 1557
25. Y. Xin, J. W. Zhao, J. Gu, S. Z. Zhu, *J. Fluorine Chem.* **132** (2011) 402
26. J. M. Indelicato, C. E. Pasini, *J. Med. Chem.* **31** (1988) 1230
27. D. J. Steenkamp, D. Weldrick, H. S. C. Spies, *Eur. J. Biochem.* **242** (1996) 566
28. K. Tanaka, T. Mori, K. Mitsuhashi, *Bull. Chem. Soc. Jpn.* **66** (1993) 263
29. S. Bigotti, L. Malpezzi, M. Molteni, A. Mele, W. Panzeri, M. Zanda, *Tetrahedron Lett.* **50** (2009) 2540
30. J. Jekowiecki, R. Loska, M. Meekelleche, *Tetrahedron* **63** (2007) 4464
31. P. Lin, J. Jiang, *Tetrahedron* **56** (2000) 3635
32. T. K. Das, S. Salampuria, M. Banerjee, *Comput. Theor. Chem.* **979** (2012) 102
33. R. G. Parr, L. V. Szentpaly, S. Liu, *J. Am. Chem. Soc.* **121** (1999) 1922
34. M. Ríos-Gutiérrez, A. K. Nacereddine, F. Chafaa, A. Djerourou, L. R. Domingo, *J. Mol. Graphics Model.* **70** (2016) 304
35. a) A. D. Becke, *Phys. Rev., A* **38** (1988) 3098; b) C. Lee, W. Yang, R. G. Parr, *Phys. Rev., B* **37** (1988) 785
36. L. Simon, J. M. Goodman, *Org. Biomol. Chem.* **9** (2011) 689
37. L. R. Domingo, M. J. Aurell, P. Pérez, *Tetrahedron* **70** (2014) 4519
38. *Gaussian 09*, Revision A.02, Gaussian, Inc., Wallingford, CT
39. W. J. Hehre, L. Radom, P. v. R. Schleyer, J. A. Pople, *Ab initio molecular orbital theory*, Vol. 7, Wiley, New York, 1986, p. 379
40. a) J. Tomasi, M. Persico, *Chem. Rev.* **94** (1994) 2027; b) B. Y. Simkin, I. Sheikhet, *Quantum chemical and statistical theory of solutions-A computational approach*, Ellis Horod, London, 1995
41. a) E. Cances, B. Mennucci, J. Tomasi, *J. Chem. Phys.* **107** (1997) 3032; b) M. Cossi, V. Barone, R. Cammi, J. Tomasi, *Chem. Phys. Lett.* **255** (1996) 327
42. a) L. R. Domingo, *RSC Adv.* **4** (2014) 32415; b) L. R. Domingo, M. Rios-Gutiérrez, P. Pérez, *Tetrahedron* **72** (2016) 1532
43. A. E. Reed, R. B. Weinstock, F. Weinhold, *J. Chem. Phys.* **83** (1985) 735
44. a) R. G. Parr, W. Yang, *Density functional theory of atoms and molecules*, Oxford, 1989; b) R. G. Parr, R. C. Pearson, *J. Am. Chem. Soc.* **105** (1983) 7512
45. R. G. Parr, L. V. Szentplay, S. Liu, *J. Am. Chem. Soc.* **121** (1999) 1922

46. a) L. R. Domingo, P. Pérez, *J. Org. Chem.* **73** (2008) 4615; b) L. R. Domingo, P. Pérez, *Org. Biomol. Chem.* **9** (2011) 7168
47. W. Kohn, J. L. Sham, *Phys. Rev.* **140** (1965) A-1133
48. L. R. Domingo, P. Pérez, J. A. Saez, *RSC Adv.* **3** (2013) 1486
49. C. Gonzalez, H. B. Schlegel, *J. Phys. Chem.* **94** (1990) 5523
50. K. B. Wiberg, *Tetrahedron* **24**(1968) 1083
51. L. R. Domingo, J. A. Saez, *Org. Biomol. Chem.* **7** (2009) 3576
52. a) R. G. Parr, W. Yang, *Ann. Rev. Phys. Chem.* **46** (1995) 701; b) H. Chermette, *J. Comput. Chem.* **20** (1999) 129
53. D. H. Ess, G. O. Jones, K. N. Houk, *Adv. Synth. Catal.* **348** (2006) 2337
54. P. Jaramillo, L. R. Domingo, E. Chamorro, P. Pérez, *J. Mol. Struct. THEOCHEM* **865** (2008) 68
55. L. R. Domingo, M. J. Aurell, P. Pérez, R. Contreras, *Tetrahedron* **58** (2002) 4417
56. L. R. Domingo, S. R. Emanian, *Tetrahedron* **70** (2014) 1267
57. H. Chemouri, S. M. Mekellecche, *Int, J. Quantum Chem.* **112** (2012) 2294.